IX Konferencja Naukowo-Techniczna – i-MITEL 2016

Michał GWÓŹDŹ, Michał KRYSTKOWIAK[1]

Politechnika Poznańska, Wydział Elektryczny,
Instytut Elektrotechniki i Elektroniki Przemysłowej, Zakład Energoelektroniki i Sterowania (1)

Three-phase diode rectifier with the current modulator based on multi-channel converter in a DC circuit

***Abstract**. In this paper a 3-phase power diode rectifier system with quasi-sinusoidal input (power grid) current is presented. In order to benefit from it, the current modulation in a DC circuit of rectifier is used. The essential part of the current modulator is a wide-band power electronics controlled current source based on a multi-channel converter. Work of a modulator control system is based on the Generalized Sampling Expansion as an extension of the Whittaker-Kotelnikov-Shannon (WKS) sampling theory. The current modulator control algorithm respects impact of aliasing phenomena at system stability using the method proposed by one of authors. The paper includes the rectifier system description and rules of work of the current modulator. Also, some results of research on both a full rectifier simulation model and a current modulator laboratory prototype are presented.*

Keywords: control methods of electrical systems, diode rectifier, Generalized Sampling Expansion, multi-channel converter, PWM

Introduction

The power rectifiers belong to a very widely utilized group of power electronics converters. Unfortunately, a standard diode and thyristor rectifier work is the reason for distortion of currents and voltages in a power grid. It has caused a very serious problem for the energetic system for many years thus, improving quality of input (power) grid current of rectifier is often necessary. A one of solutions obtaining it is rectifier based on using a passive or active filter at the input [1,2]. The following way relies on using of so call “active rectifier”, which is built with transistor (IGBTs) inverter switched at frequency which is several times higher than frequency of voltage source in a power grid [3]. Also, to correct the waveform of the power grid current the rectifier built with diodes (or thyristors) being interconnected by means of coupled inductors can be used [4]. Another, an advanced solution of rectifier system, includes of a voltage modulator in the DC circuit of the rectifier. The modulator is built with thyristors and a special inductor with several taps. It has been considered e.g. in [5].

All mentioned solutions are relatively expensive ones. Thus, in this paper another possible solution being able to shape the waveform of power grid current toward the sinusoidal waveform is presented. This one is based on the current modulation in the DC circuit [5, 6]. Such a rectifier system is built with two 6-pulse diode rectifiers, which are supplied by two 3-phase transformers with the connection star-star and star-delta. In this way 30 el. deg. phase shift of transformers output voltages is obtained. Additionally, in a DC circuit a special power electronics converter called a “current modulator” is placed. The current modulator is responsible for shaping of the rectifier input currents – Fig. 1. In fact the star-star connected transformer is not necessary for proper work of the modulator although it helps to scale the voltage levels of both rectifiers in the laboratory prototype of the rectifier system [5].

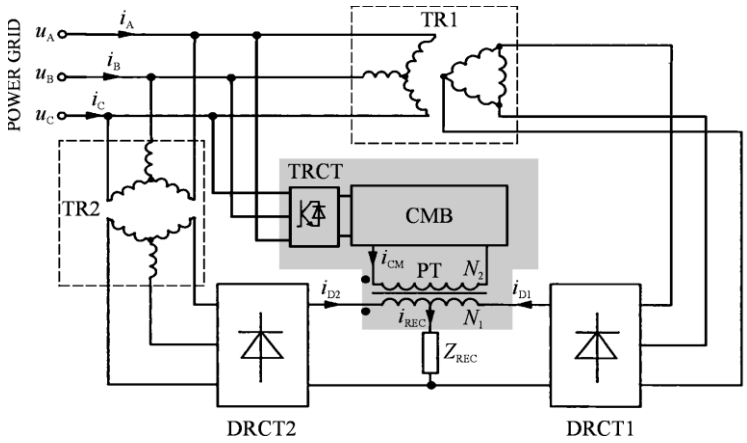

Fig. 1. General block diagram of the 3-phase diode rectifier with the current modulator in a DC circuit.

The rectifier system consists of the following blocks: two transformers connected in the star-delta (TR1) and star-star (TR2) manner, two standard 6-pulse diode rectifiers (DRCT1 and DRCT2) with DC circuits connected in parallel, the active (transistor) rectifier (TRCT) and the current modulator block (CMB). The CMB is connected to the DC circuit across the pulse transformer (PT). Rectifiers power a common receiver, expressed by Z_{REC}. The current modulation conception assumes a very large time constant of the receiver impedance. Similarly like the TR2 transformer, the transistor rectifier is not necessary in the rectifier circuitry too. Its role depends on control the voltage level in the DC link of the modulator only – without any impact on the modulator output current [5]. Thanks to this rectifier input currents are better matched in the sinusoidal waveform.

The presented solution of the rectifier system makes it possible to improve significantly the quality of rectifier power grid currents i_{A}, i_{B} and i_{C}. I.e. waveforms of these are close to the sinusoidal shape. The current modulator works as a power electronics controlled current source being connected to the DC circuit of rectifiers across a wide-band pulse transformer with two taps on a primary site. The i_{CM} output current of the modulator is added (with a sign of “plus” or “minus”), with the aid of the PT, to the output current i_{D1} and i_{D2} of each rectifier in terms of the following equations:

$$(i_{\mathrm{D2}}-i_{\mathrm{D1}})N_1=i_{\mathrm{CM}}N_2$$

$$i_{\mathrm{D1}}=\frac{1}{2}\left(i_{\mathrm{REC}}-\frac{N_2}{N_1}i_{\mathrm{CM}}\right) \quad (1)$$

$$i_{\mathrm{D2}}=\frac{1}{2}\left(i_{\mathrm{REC}}+\frac{N_2}{N_1}i_{\mathrm{CM}}\right)$$

where, equation quantities are as follows: $\frac{N_1}{N_2}$ – the PT windings turn ratio, i_{REC} – the receiver current and i_{CM} – the CMB output current.

This is the way in which waveforms of input currents of two rectifiers are modified. In consequence, resultant waveforms of power grid currents of the rectifier system (i_{A} , i_{B} , and i_{C}) are modified as well. The power of each, the active rectifier and the current modulator is only 2÷3 % of the total power at the output of the DC circuit. This is a great advantage of this idea of the rectifier system. Thanks to utilization of an active rectifier the resultant system energy efficiency is somewhat improved too. What is also important, in case of disabling of the modulator (e.g. due to damage of it) a system is able to continue its work as a standard 12-pulse diode rectifier.

In order to obtain the sinusoidal shape of the power grid current, the modulator current i_{CM} should satisfy the following equation [6]:

(2)

$$i_{\mathrm{CM}}(t)=\frac{\sqrt{3}\frac{2\sqrt{3}}{\pi}I_{\mathrm{REC}}\cos\left(\omega_{\mathrm{g}}t\right)-I_{\mathrm{REC}}\left[\cos(6k\omega_{\mathrm{g}}t)+\cos(6k\omega_{\mathrm{g}}t+\frac{\pi}{6})\right]}{-\cos(6k\omega_{\mathrm{g}}t)+\cos(6k\omega_{\mathrm{g}}t+\frac{\pi}{6})}\frac{N_1}{N_2}:k=0,1,2,...$$

However, the complex current form of the equation (2) can be replaced by a current with triangular shape, with only a small deterioration of the THD factor of a rectifier input current [6]. The fundamental frequency of the modulator current has to be equal to 6-times of power grid frequency, i.e. 300 Hz:

(3) $$i_{\mathrm{CM}}(t)=\frac{4}{\pi}I_{\mathrm{REC}}\left[\sin(6\omega_{\mathrm{g}}t)-\frac{\sin(3\,6\omega_{\mathrm{g}}t)}{3^2}+\frac{\sin(5\,6\omega_{\mathrm{g}}t)}{5^2}-...\right]$$

where ω_{g} is the fundamental frequency of the voltage in the power grid.

With such replacement, assuming the power grid is a symmetrical one, a THD factor of a power grid current is equal to about 1% [5, 6]. Thus, the current modulator has to include in its own structure a wide-band power electronics controlled current source which would be able to match precisely an output (modulator) current in the reference signal [7]. This feature of the modulator is essential for proper working of the rectifier system because it determines directly the quality of its input current.

Initially, in the current modulator the standard (i.e. one-channel) inverter has been implemented. This one has been a part of the laboratory prototype of rectifier system [5]. The present article is focused mainly on utilizing in a current modulator a wide-band power electronics controlled current source based on a multi-channel (interleaved) converter [8, 9].

The whole text is divided into 6 sections. The first one deals with the general rectifier conception. The second one shows a basic description of the wide-band power electronics controlled current source based on a multi-channel converter. In the third section, an issue of controlled source stability is considered. The fourth section presents mainly, among other items, a simulation model of the rectifier system. In the fifth section

selected results of research on a laboratory prototype of the current modulator are presented. The last part is dedicated to conclusions.

Wide-band power electronics controlled current source

Dynamic changes of parameters of energy sources and receivers are the reasons for decreasing exactitude of output signals towards reference signals. In order to improve these parameters often more advanced solutions of power electronics converters are necessary. They can be exemplified by a wide-band power electronics voltage controlled voltage source (VCVS) or voltage controlled current source (VCCS). Such a converter should match an output signal precisely in a reference waveform so that both a modified electrical structure of a converter and an effective control algorithm are necessary. It has many applications in a power electronics equipment.

In Fig. 2 a general structure of the VCCS is shown. It is based on the conception of a multi-channel converter where a i_{L} total output current is proportional to the sum of currents $i_{\mathrm{L},i} : i = 0,1,...,M-1$ in individual channels of a converter.

The VCCS is a system which works in a closed, voltage type, negative feedback loop. Inverters in an execution block of the VCCS are controlled in PWM mode with the constant value of a carrier frequency [7]. One of the fundamental blocks of the VCCS is a passive low-pass filter at the output of power stage consisting of a set of connected in parallel inductors. This filter has two basic tasks to do, namely it obtains the suitable value of the output impedance of a converter and minimizes amplitude of PWM carrier components in the output current, making it possible for the converter to meet requirements of EMC.

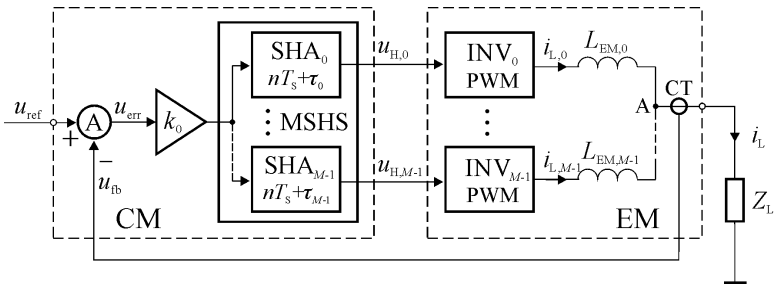

Fig. 2. Block diagram of the VCCS.

The general structure of the VCCS is based on two modules, the control module (CM) and the execution module (EM). The control module includes the following internal blocks:

- adder (A), producing the error signal $u_{\mathrm{err}} = u_{\mathrm{ref}} - u_{\mathrm{fb}}$,
- regulator of the output current with the gain factor of k_0,
- M-order multi-dimensional sample-and-hold system (MSHS) consisting of M connected in parallel sample-and-hold amplifiers.

The execution module consists of:

- M-connected in parallel half-bridge type inverters,
- output filter ($L_{\mathrm{EM},i} : i = 0,1,...,M-1$),
- current transducer (CT), producing the feedback voltage u_{fb}, being proportional to the VCCS output current i_{L}.

The EM is loaded by the Z_{L} impedance and $Z_{\mathrm{L}} = \mathrm{j}\omega L_{\mathrm{L}} + R_{\mathrm{L}}$. The VCCS is controlled by the reference voltage u_{ref} at the input of the CM.

The sampling moments and PWM carrier signals in individual channels of the converter are shifted with each other by $\frac{T_{\mathrm{s}}}{M}$, where T_{s} is a master sampling period. In result, from the point of view of system stability, the converter "transfer function" is preferably modified [10]. Thanks to this, the regulator gain in the VCCS control system can be increased compared to an one-channel converter. It has a very positive impact on the performance of the VCCS because a control algorithm lets more accurately match the VCCS output current in a reference one.

Owing to shifting also by time $\frac{T_{\mathrm{s}}}{M}$ of carrier signals in individual channels of the EM the effective carrier frequency in the output signal is shifted M-times towards higher frequencies. In consequence, the amplitude of current ripples in the converter output current, caused by pulse modulation, is reduced significantly as well.

In this particular case of work of the VCCS in a rectifier system, the structure of the VCCS has been slightly modified. It has been necessary due to way of including the pulse transformer in this system based on a *virtual ground*. As a result, the 2x2-channel modified inverter in the EM of the VCCS has been used. The block scheme of the VCCS is presented in Fig. 3.

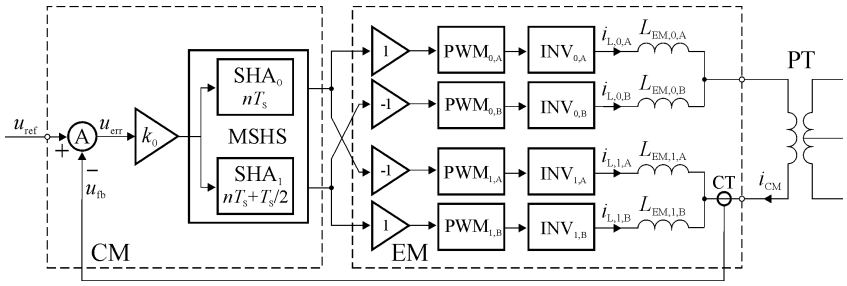

Fig. 3. Block diagram of the VCCS for driving the pulse transformer.

The modulation used in pulse modulators is two-sided and asymmetric. The load of the VCCS – the pulse transformer – is included in the circuit in a differential manner. I.e. voltage at the output of the $\mathrm{INV}_{0,x}$ inverters pair has to be in anti-phase with respect to the voltage at the output of the $\mathrm{INV}_{1,x}$ pair. Because of M =2, sampling moments in the SHA_1 and SHA_0 should be shifted with each other by a $\frac{T_{\mathrm{s}}}{2}$ time.

Taking into account the pulse modulation parameters mentioned above, the T_{c} period should be equal to $2T_{\mathrm{s}}$ and carrier signals in a $\mathrm{PWM}_{x,\mathrm{A}}$ modulator and in a $\mathrm{PWM}_{x,\mathrm{B}}$ modulator should be shifted with each other by a time $\frac{T_{\mathrm{c}}}{4} = \frac{T_{\mathrm{s}}}{2}$.

Stability issue of a controlled current source

One of the most important aspects of the current modulator work is its stability. This analysis will include an important factor that occurs in the operation of a real system, which usually is not respected. This is an aliasing phenomenon – characteristic for sampled-data systems. The mathematical model of a control system of a multi-channel converter for the stability analysis has been proposed e.g. in [10]. This description is based on the extension of Whittaker-Kotelnikov-Shannon (WKS) sampling theory – the Generalized Sampling Expansion (GSE) – being formulated by Papoulis [11].

Assume signal $x(t) \in \mathrm{L}^2(\Re)$, the space of square-integrable functions, where $\Re$ – real numbers domain, and its Fourier transform $X(\mathrm{j}\omega)$ exists. Assume also that sampling of $x(t)$ is uniform and ideal (i.e. with utilization of Dirac series $\sum_n \delta(t - nT_\mathrm{S}) : T_\mathrm{S} \le \frac{\pi}{\omega_\mathrm{MAX}}$, where T_S is the sampling period) and $y(t)$ is the signal at output of a sample-and-hold amplifier (SHA) as an 0-order extrapolator of a sampled signal. The relationship between $X(\mathrm{j}\omega)$ and $Y(\mathrm{j}\omega)$ apart a *static* (time invariant) component, also contains a *dynamic* (time variant) component $\sum_{n=-\infty}^{\infty} X\left[\mathrm{j}\left(\omega - n\frac{2\pi}{T_\mathrm{S}}\right)\right]$, so the formal transfer function of the SHA does not exist. The *dynamic* component is also related to the aliasing effects, by which the high frequency poles are folded back into lower frequencies. Although respecting the *static* part only of equivalent transfer function of SHA gives, in most cases of the system stability analysis, satisfying results, the crucial knowledge is that the aliasing mechanism can cause loss of stabilization at critical frequencies [10,12,13,15].

From the point of view of the GSE, general setting is that a signal $x(t)$ is processed by a linear multi-dimensional sampling system (MSS). Suppose now that $x(t)$ is a common input to M sampling systems and each individual sampling system is a sub-system of the MSS – Fig. 4.

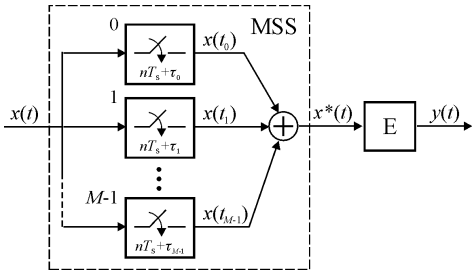

Fig. 4. MSS with a single ZOH block as a signal extrapolator (E) at the output.

Each sub-system samples at a rate of $\frac{1}{M}$ times of the Nyquist rate. Assuming individual delay $\tau_i = i\frac{T_\mathrm{S}}{M} : i = 0,1,...,M-1$, the $x(t)$ can be retrieved from its samples $x^*(t)$ by using the inverse Fourier transform formula:

$$x(t)=\frac{1}{2\omega_{\mathrm{MAX}}}\sum_{n=-\infty}^{\infty}\sum_{i=0}^{M-1}\left\{x\left[\left(n+\frac{i}{M}\right)T_{\mathrm{s}}\right]\int_{-\omega_{\mathrm{MAX}}}^{\omega_{\mathrm{MAX}}}\mathrm{e}^{\,\mathrm{j}\omega\left[t-\left(n+\frac{i}{M}\right)T_{\mathrm{s}}\right]}\mathrm{d}\omega\right\} \tag{4}$$

The overall sampling rate still satisfies the Nyquist criterion [11]. The MSS, being the consequence of GSE, makes it possible to reduce the required sampling frequency to $\frac{1}{M}$, comparing to one-dimensional sampling system (WKS sampling theorem), working at the same sampling rate. Considering the system from the other side, when it sampling at a rate of $\frac{1}{T_{\mathrm{s}}}$ its effective sampling rate is equal to $\frac{M}{T_{\mathrm{s}}}$. A Nyquist band is now M -times extended. In the case of a control system of a real multi-channel converter an essential difference in relation to GSE assumption appears. It consists in the fact that each individual converter channel includes a single SHA and individual channels output signals are summed at the output of the converter. This modification of the original GSE concept is necessary due to the different position in the system of a signals summing node. The second reason results from the limitation of dynamic parameters of real power electronics devices used in inverters. In other words, switching frequency has to be limited due to energy loss in transition states of power electronics switches. Thus, the VCCS control system includes now the multidimensional sample-and-hold system (MSHS) instead of the MSS [10]. The proposed small-signal (linear) model of the VCCS with the 2nd order MSHS, being the object of further considerations, is shown in Fig. 5.

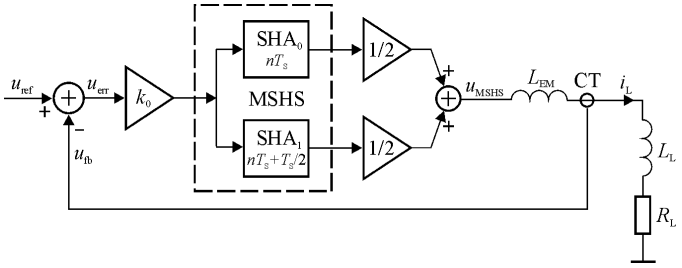

Fig. 5. Small-signal model of the VCCS based on a 2-channel converter.

The proposed model is an IOM, SISO and LTI one and can be completely described in terms of a continuous-time system with a transfer function $G(\mathrm{j}\omega)=\frac{I_{\mathrm{L}}(\mathrm{j}\omega)}{U_{\mathrm{ref}}(\mathrm{j}\omega)}=\frac{K(\mathrm{j}\omega)}{1+K_{\mathrm{al}}(\mathrm{j}\omega)}$. The system stability analysis takes advantage of Nyquist criterion [14]. Hence, a characteristic equation $R(\mathrm{j}\omega)=1+K_{\mathrm{al}}(\mathrm{j}\omega)=0$ of the model, respecting (4), takes the following form:

$$R(\mathrm{j}\omega)=1+r_{\mathrm{CT}}k_0\sum_{n=-N_{\mathrm{MAX}}}^{N_{\mathrm{MAX}}}\frac{K_{\mathrm{MHS}}\left[\mathrm{j}(\omega-n\omega_{\mathrm{s}})\right]}{\mathrm{j}(\omega-n\omega_{\mathrm{s}})(L_{\mathrm{EM}}+L_{\mathrm{L}})+R_{\mathrm{L}}}=0 \tag{5}$$

where: $K_{\mathrm{MHS}}(\mathrm{j}\omega)$ – a static component in a relationship of the MSHS input and output signals, r_{CT} – the gain factor of CT, k_0 –gain of the regulator, $\omega_{\mathrm{s}} = \dfrac{2\pi}{T_{\mathrm{s}}}$ – a sampling frequency and N_{MAX} is a number of respected aliases. The function (7) possesses $2N_{\mathrm{MAX}}+1$ singular points at the frequency $\omega = n\omega_{\mathrm{s}}$.

Research of the VCCS small-signal model have defined the static component in the relationship of input and output signals of the MSHS as follows:

$$(6)\quad K_{\mathrm{MHS}}(\mathrm{j}\omega) = \begin{cases} \mathrm{Sa}\left(\omega\dfrac{T_{\mathrm{s}}}{2}\right)\mathrm{e}^{-\mathrm{j}\omega\frac{T_{\mathrm{s}}}{2}} : \ M = 1 \\ \mathrm{Sa}\left(\omega\dfrac{T_{\mathrm{s}}}{2}\right)\cos(\omega a T_{\mathrm{s}})\mathrm{e}^{-\mathrm{j}\omega\frac{T_{\mathrm{s}}}{2}} : \ M = 2, a = \dfrac{1}{2}\dfrac{\tau_0-\tau_1}{T_{\mathrm{s}}} \wedge a \in \left\langle -\dfrac{1}{4}, \dfrac{1}{4}\right\rangle \\ \mathrm{Sa}^2\left(\omega\dfrac{T_{\mathrm{s}}}{2}\right)\mathrm{e}^{-\mathrm{j}\omega\frac{T_{\mathrm{s}}}{2}} : \ M \to \infty \end{cases}$$

The Nyquist diagram for the general form of the equation (5) i.e. $R(\mathrm{j}\omega) = 1 + K_{\mathrm{al}}(\mathrm{j}\omega)$, respecting (8), is shown in Fig. 6. It concerns the following exemplary parameters of the small-signal model: r_{CT} =1 V/A, $L_{\mathrm{EM}} + L_{\mathrm{L}}$ =5 mH, R_{L} =0, T_{s} =50 μs and k_0 =120. Since the general form of the equation (5) is a periodic function in ω with the period of T_{s}, the (P,Q) diagram is also periodic in intervals $\left\langle n\dfrac{2\pi}{T_{\mathrm{s}}}, (n+1)\dfrac{2\pi}{T_{\mathrm{s}}}\right\rangle : -N_{\mathrm{MAX}} \le n \le N_{\mathrm{MAX}}$.

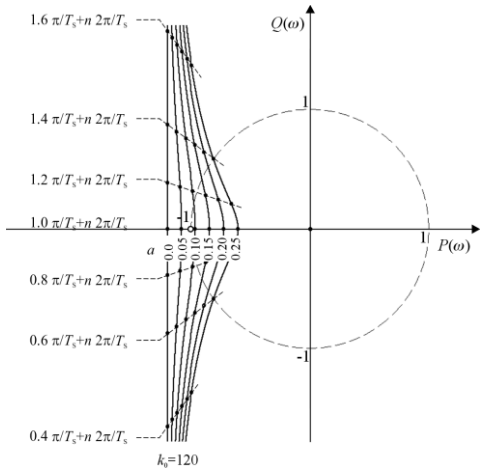

Fig. 6. Nyquist diagram for the characteristic equation of the small-signal model of the VCCS while M =2 and a =var.

For the mentioned-above hypothetical model parameters and exemplary cases of the a factor: 0.10, 0.15, 0.20 and 0.25, the (P,Q) phase curve encircles the Nyquist point on the right side indicating that the system is stable. The characteristic effect of the 2nd order sampling is decreasing gain of the MSHS while frequencies are close to the Nyquist frequency. The gain minimizing effect is maximal whereas sampling is orthogonal (i.e. a =±1/4) [10].

It is very interesting and crucial for further utilization of multi-channel inverter concept to determine the maximal regulator gain (k_0) to make the system stable. In order to determine this value it is necessary to determine amplitude of $K_{\mathrm{al}}(\mathrm{j}\omega)$ for the critical phase value $\arg\{K_{\mathrm{al}}(\mathrm{j}\omega)\} = \pm\pi$. It occurs for the frequency $\omega_{\pi,n} = (2n+1)\frac{\pi}{T_{\mathrm{s}}} : n = 0,\pm1,\pm2,...$. Having solved the equation (5), the maximal regulator gain can be expressed by the following formula:

$$k_{0,\mathrm{MAX}} < \begin{cases} \dfrac{L}{r_{\mathrm{CT}} T_{\mathrm{s}}} : M = 1,\ M = 2 \wedge a = 0 \\ 2\dfrac{L}{r_{\mathrm{CT}} T_{\mathrm{s}}} : M = 2 \wedge a = \pm 1/4 \end{cases} \tag{7}$$

where $L = L_{\mathrm{EM}} + L_{\mathrm{L}}$.

The maximal theoretical value of the regulator gain occurs in the case of M =2 and a =±1/4. It is 2-times over the gain of the regulator in case of a one-channel converter. It gives higher quality matching a VCCS output current in a reference signal. First of all, this case of the VCCS control system parameter will be taken into account in the final considerations. The response of the VCCS small-signal model for the square-wave reference signal is shown in Fig. 7. The regulator gain is close to the maximal value – in terms of the expression (7) and model parameters listed earlier.

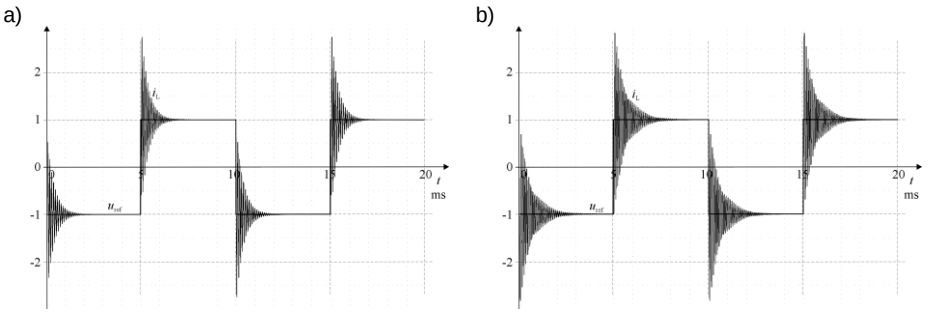

Fig. 7. Waveforms of characteristic signals – the output current i_{L} and the reference voltage u_{ref} – in the small-signal model of the VCCS while: a) M =1 (or: M =2, a =0), k_0 =95 and b) M =2, a =1/4, k_0 =190.

As it can be observed, both systems are close to the un-stability boundary but the value of the regulator gain in case of a two-channel converter is twice over a gain of a standard converter.

Simulation model of the rectifier system

A complex simulation model of the 3-phase 12-pulse diode rectifier system with the current modulation in the DC circuit has been investigated in detail. The fundamental block of the current modulator is the VCCS based on a 2-channel converter. The 2nd-order MSHS has been used in the current regulator. In many cases, the results of the study also relate to the VCCS based on a one-channel converter for comparison parameters of both systems.

Selected waveforms in the simulation model for the target shape (i.e. triangular) of the reference signal are shown in the following Figure. These are also related to the two cases of an order of the MSHS i.e. M =1 and M =2. The PWM carrier frequency T_c =100 μs, a PWM kind is two-sided and asymmetric, the nominal amplitude value of the reference voltage $A_{ref,n}$ =10 A, and $L_{EM,0,A} = L_{EM,0,B} = L_{EM,1,A} = L_{EM,1,B}$ =1.2 mH. Values of parameters of the simulation model are consistent with parameters of the real system, which is described in the next section.

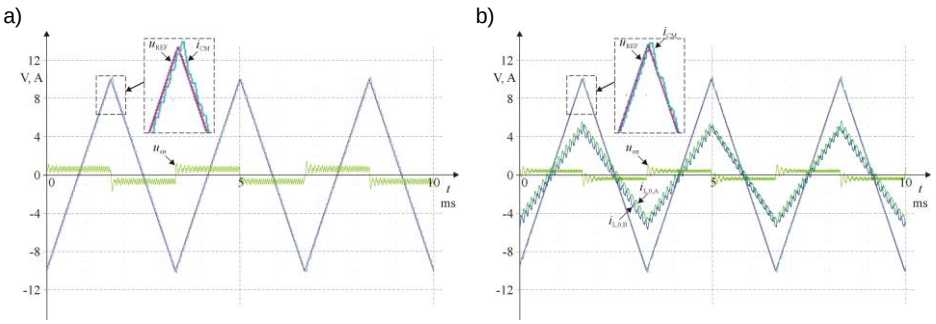

Fig. 8. Waveforms of the reference voltage u_{ref} , modulator current i_{CM} , and the error signal u_{err} for the case of triangular shape of reference signal and: a) M =1, k_0 =35, b) M =2, a =1/4, k_0 =40. Also currents in individual channels of the VCCS ($i_{L,0,A}$ and $i_{L,0,B}$) are shown – Fig. b). Amplitude of the reference signal is equal to the nominal one.

In the case of the two-channel VCCS shapes of the modulator current and reference signal almost coincide, in contrast to the standard VCCS, where these signals clearly differ from each other. For the VCCS in a two-channel version the first pulse modulation component in the modulator current is at $\frac{4}{T_c}$ frequency, instead of $\frac{2}{T_c}$ and its amplitude is over 3-times lower compared to a one-channel converter.

A very adequate and reliable criterion of the quality of a converter output signal can be the converter control error given by the following equation:

(8) $$\varepsilon_{CTR} = \sqrt{\frac{\overline{|u_{err}|^2}}{|u_{ref}|^2}} 100\% = \sqrt{\frac{\overline{|u_{ref} - u_{fb}|^2}}{|u_{ref}|^2}} 100\%$$

Assuming nominal conditions of the simulation model work, the value is as follows: $\varepsilon_{\mathrm{CTR}}$ =5.88 %: M =1, $\varepsilon_{\mathrm{CTR}}$ =3.63 %: M =2. Thus, in sense of this criterion a two-channel VCCS makes it possible to improve the quality of the output current about 62 % compared to a one-channel VCCS solution.

The research on the rectifier system has been based mainly on its simulation model in the ORCAD/PSpice environment. The basic electrical structure of the model is introduced in Fig. 9. It respects all fundamental features of an exemplary real system, e.g. non-zero power grid impedance, non-zero windings resistance and leakage inductances of power transformers and the pulse transformer [16]. Also, switching processes in rectifier diodes and in IGBTs used in the inverter, being execution part of the VCCS, are respected. However, the active rectifier (the TRCT block) has not been taken into consideration. The simulation model has been "powered" by 3x230 V, 50 Hz grid. The nominal DC output power of the rectifier system $P_{\mathrm{DC,n}}$ has been set at 6 kW.

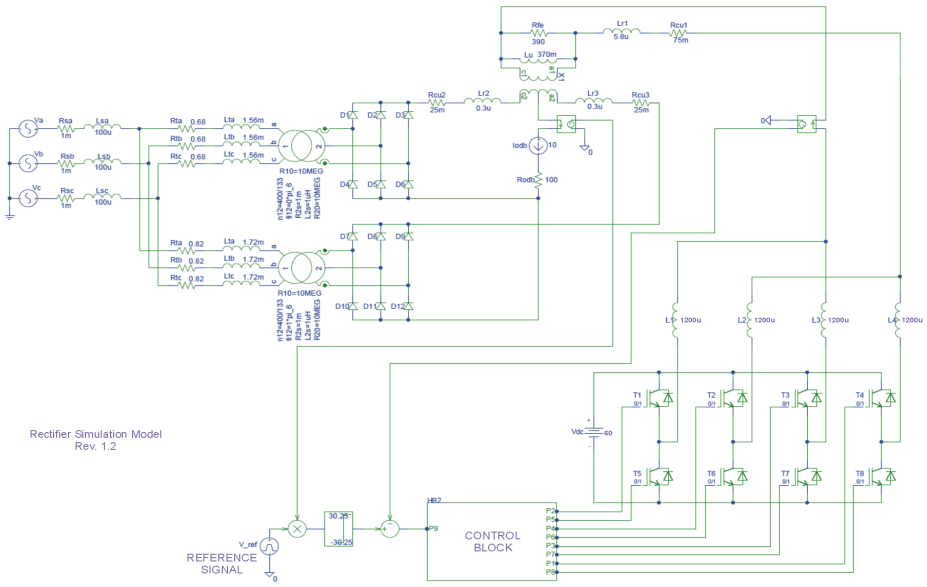

Fig. 9. Rectifier system simulation model (the main block) in the ORCAD/PSpice environment.

The following Figure is a typical one. It presents power grid currents in a standard 12-pulse diode rectifier and, also, in the introduced rectifier system while a current modulator is disabled. In accordance with the listed parameters of the rectifier simulation model and the nominal output power, the THD value for the power grid current (i_{A}, i_{B} and i_{C}) is approx. equal to 12.5 % in a 5 kHz band.

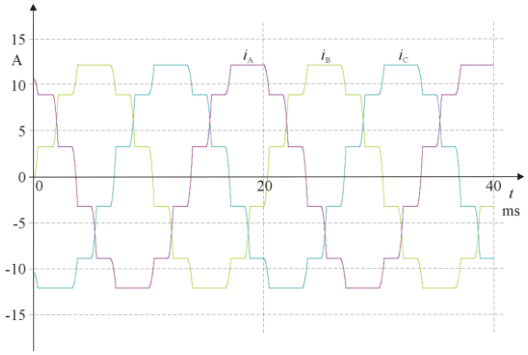

Fig. 10. Waveforms of power grid current i_A, i_B and i_C in the rectifier simulation model while the output power is equal to nominal one and the current modulator is disabled.

In Fig. 11, in contrast to the previous situation, the current modulator is enabled. In results, deformations of power grid currents are now of an over order less i.e. THD =1.35 % while the output power is equal to the nominal value and THD =2.93 % while the output power is equal to the 10% of this one.

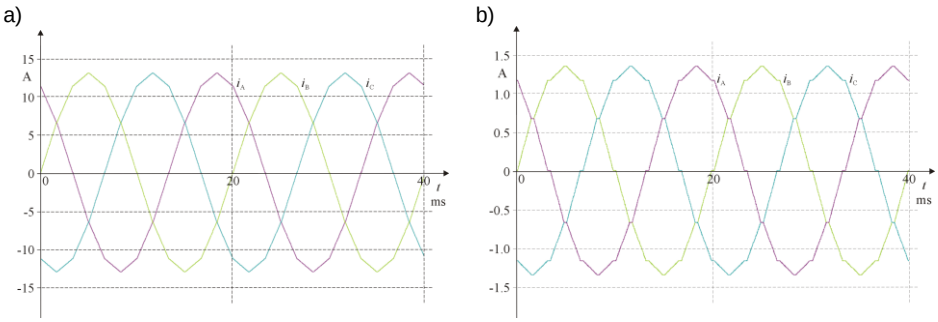

Fig. 11. Waveforms of power grid currents i_A, i_B and i_C in the rectifier simulation model while the current modulator is enabled and: a) the output power is equal to the nominal value, b) the output power is equal to 10% of the nominal value.

The impact of the number of converter channels on the quality of power grid currents can be evaluated on the basis of the ε_i error. This one is related to the difference of a i_A (i_B, i_C) current and its 1st harmonics – similarly to the converter control error (10). A value of this error is function of both, the rectifier output power P_{DC} and M: $\varepsilon_{i,M} = f\left(\frac{P_{DC}}{P_{DC,n}}\right) : M = 1, 2$. The graph of this function is shown in Fig. 12. Also, the relationship of $\varepsilon_{i,2}$ and $\varepsilon_{i,1}$ is presented.

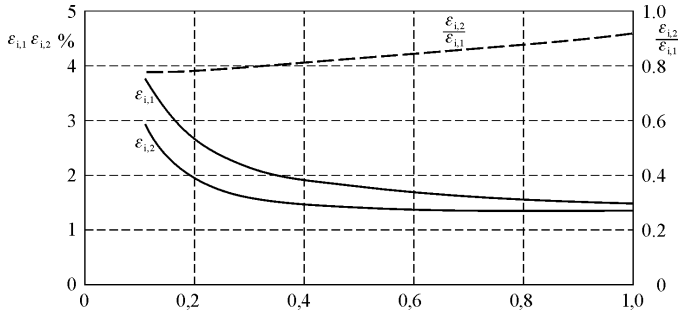

Fig. 12. Curves of ε_{i} and a reciprocal relationship of error functions while M =1 and M =2.

The quality of the power grid current in case of utilization of the two-channel converter is increased about 10.8÷28.3 % compared to the standard one, while its average value is approx. equal to 11.8 %. In consequence, power loss in the rectifier system (mainly in transformers) can be reduced by means of a two-channel converter solution.

The next Figure presents spectrum of the power grid voltage u_{A} (u_{B} and u_{C}) for two cases of the VCCS solution – based on a one-channel and a two-channel converter.

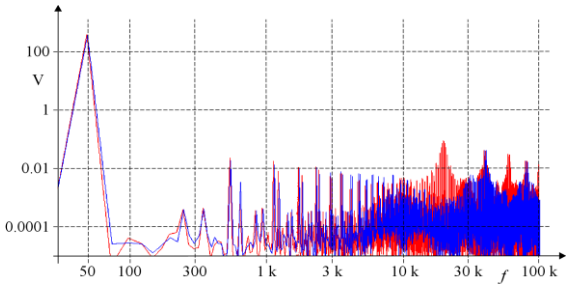

Fig. 13. Spectrum of the power grid voltage u_{A} (u_{B}, u_{C}) while M =1 (the red curve) and M =2 (the blue curve).

In the case of the two-channel VCCS pulse modulation components in the input voltage spectrum are shifted at $2if_{\mathrm{c}} : i \in \mathrm{C}$ frequencies, compared to the one-channel converter. It gives minimization of the level of disturbances in the power grid so the current modulator as power electronics converter can meet EMC requirements more easily.

Laboratory model of the current modulator

Also, the laboratory model of the part of rectifier system has been investigated. The aim of the study has been validation of theoretical assumptions and research results of the rectifier simulation model – mainly in the relation to the quality of the modulator current. The laboratory model has consisted of these blocks of the full rectifier circuitry which are on the grey background in Fig. 1. Its diagram has been consistent with Fig. 3. The secondary winding of the pulse transformer has been short circuited.

Basic technical parameters of the laboratory prototype are given below:

- DC link voltage in the multi-channel converter: 60 V,
- nominal amplitude of the modulator current: 10 A,
- inductance of the single choke in the VCCS: 1.15÷1.27 mH,
- signal sampling frequency in the control module: 20 kHz,
- PWM carrier frequency: 10 kHz,
- mode of the PWM generator work: double-updated (per the carrier period).

Pulse transformer parameters are shown in Fig. 9. These have been determined on the basis of measurements of the real transformer [16] which has been implemented in the first laboratory model of the rectifier system [5]. The general view of the laboratory stand is shown in Fig. 14.

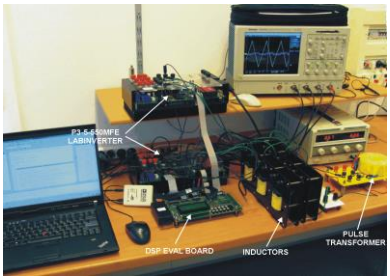

Fig. 14. General view of the laboratory stand.

The control module in the laboratory prototype has been based on the ALS-G3-1369 DSP evaluation board with Analog Devices ADSP-21369 SHARC® DSP while in the execution block two P3-5-550MFE LABINVERTERs have been utilized. This family of DSP is equipped with the high performance 16-channel PWM generator hence, is especially dedicated implementation in power electronics devices. Also the LABINVERTER development system is designed for applications in a power electronics; it is equipped, among other items, with a 3 legs IPM/IGBT. Both of these systems are manufactured by ALFINE-TIM [17]. In order to observe and analyze waveforms the TEKTRONIX DPO5034B oscilloscope has been used.

Laboratory model tests have been carried out for the current modulator amplitude being in the range of 10 %÷100 % of the nominal one. Also, two cases of converter configuration have been tested i.e. M =1 and M =2. In Fig. 15 and 16 selected waveforms in the laboratory prototype of the modulator system are shown.

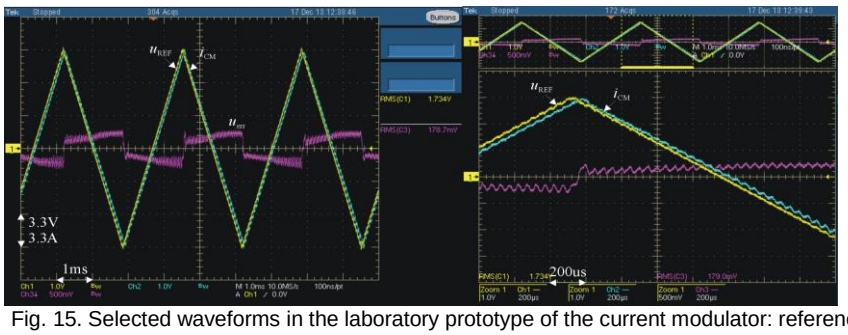

Fig. 15. Selected waveforms in the laboratory prototype of the current modulator: reference voltage, modulator current, and error signal while M =1. The current modulator amplitude is equal to the nominal one.

a)

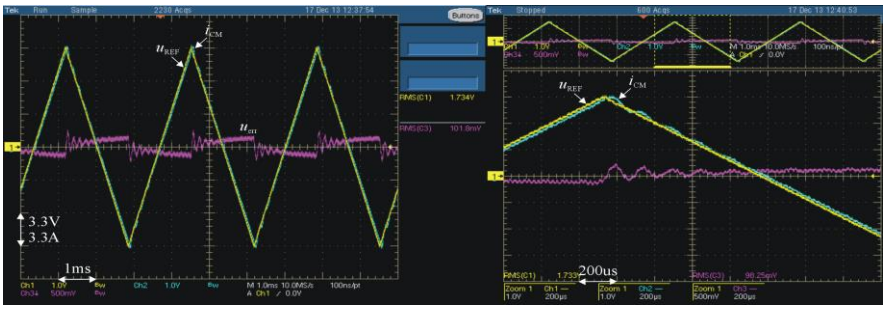

b)

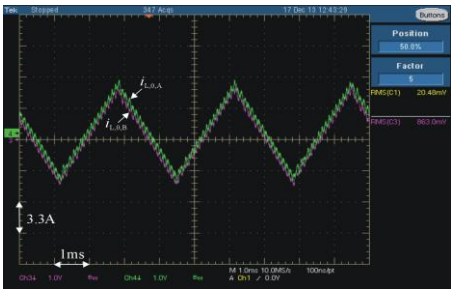

Fig. 16. Selected waveforms in the laboratory prototype of the current modulator: reference voltage, modulator current, error signal – Fig. a), and currents in individual channels of the VCCS – Fig. b), while M =2. The current modulator amplitude is equal to the nominal one.

Assuming nominal conditions of the laboratory model work, the value of the control error is as follows: $\varepsilon_{\mathrm{CTR}} \cong$9.8 %: M =1 and $\varepsilon_{\mathrm{CTR}} \cong$5.9 %: M =2. Thus, in sense of the control error criterion a two-channel VCCS makes it possible to improve the quality of the output current about 66 % compared to a one-channel VCCS solution. Higher (compared to the simulation model) the control error value is caused mainly by errors (non-linearity) of current transducers, which e.g. the total accuracy is equal to 0.65 %. Also, inductors and pulse transformer based on ferromagnetic (respectively powdered iron and silicon steel) cores are non-linear. However, in this case the relationship of the control error values is similar to the case of the simulation model. In the authors opinion it confirms the good quality of the simulation model.

Conclusions

In this study one of the ways leading to increasing the quality of power grid current of traditional diode rectifiers is presented. In order to obtain this a current modulator in the common DC circuit of two 6-pulses rectifiers has been utilized. The modulator is based on a wide-band power electronics controlled current source with a multi-channel converter. The converter control system implements assumptions of the Papouli's Generalized Sampling Expansions theory. Also, the control algorithm respects aliasing effects, having the influence on the system stability, taking place in sampled-data systems. They make it possible to maximize crucially effective gain of the regulator and, in consequence, better matching of the modulator output current in the reference signal.

As a result the total THD factor of the power grid current is lowered approx. 11%÷28%, compared to the standard converter. It gives opportunity of decreasing power losses in the rectifier power grid transformers. Thanks to features of a multi-channel converter the spectrum of the power grid voltage is more beneficial due to PWM components are shifted at the higher frequency zone.

The solution of a rectifier is especially attractive in the case of a higher power of the receiver, since power of the current modulator is approx. equal to 2÷3 % of the rectifier DC output power. Thus, higher complexity of the proposed converter solution has only a minimal effect on the cost of the whole rectifier system.

Also, in the nearest future it is planned the full construction of a laboratory model of the rectifier system. It will be done in cooperation with an industrial partner. This model can be treated as an extension of the current modulator prototype based on a two-channel converter.

References

1. M. Siwczyński and M. Jaraczewski, "Reactive compensator synthesis in time-domain", *BULLETIN OF THE POLISH ACADEMY OF SCIENCES TECHNICAL SCIENCES*, Vol. 60, No. 1, 119-124 (2012).
2. M. Gwóźdź, "Power Electronics Active Shunt Filter with Controlled Dynamics", *Proc. of COMPEL: The International Journal for Computation and Mathematics in Electrical and Electronic Engineering*, Vol. 32, No. 4, 1337-1344 (2013).
3. M. Jasiński, P. Antoniewicz and M. P. Kaźmierkowski, "Induction Motor Drive fed by PWM Rectifier/Inverter with Victor Control" (in Polish), *Przegląd Elektrotechniczny*, No 6/2005, 1-5 (2005).
4. P. Mysiak and R. Strzelecki, "A robust 18-pulse diode rectifier with coupled reactors", *BULLETIN OF THE POLISH ACADEMY OF SCIENCES TECHNICAL SCIENCES*, Vol. 59, No. 4, 541-550 (2011).
5. M. Krystkowiak, *Power rectifier system with improved rates with power electronics current modulator* (in polish), *Doctoral thesis*, Poznan University of Technology, Faculty of Electrical Engineering, Poznań (2009).
6. R. Strzelecki and H. Supronowicz, "The power factor of AC circuits and correction method" (in polish), OWPW, Warszawa, 120–135 (2000).
7. M. Gwóźdź, "Analysis of work of wide-band power electronics converters" (in polish), *Przegląd Elektrotechniczny*, No 12, 216-221 (2010).
8. S. Huth, "DC/DC converters in Parallel Operation with digital load distribution control", *Proceedings of the IEEE International Symposium on Industrial Electronics*, Vol. 2, 808-813 (1996).
9. L. Asiminoaei, E. Aeloiza, P.N. Enjeti, and F. Blaabjerg, "Shunt Active-Power-Filter Topology Based on Parallel Interleaved Inverters", *IEEE TRANSACTIONS ON INDUSTRIAL ELECTRONICS*, Vol. 55, No. 3, 1175 - 1189 (2008).
10. M. Gwóźdź, "Stability of Discrete Time Systems on Base Generalized Sampling Expansion", *Kwartalnik Elektryka*, Politechnika Śląska, Vol. 1 (217), Gliwice, 29-40 (2011).
11. A. Papoulis, "Generalized Sampling Expansion", *Proceedings of the IEEE Transactions on Circuits and Systems*, Vol. 24, Issue 11, 652 - 654 (1977).
12. L. Mirkin and Z. J. Palmor, "Control Issues in Systems with Loop Delays", *The Handbook of Networked and Embedded Control Systems* (D. Hristu-Varsakelis and W. S. Levine, eds.), Birkhäuser, 627–648 (2005).
13. G. Meinsma and L. Mirkin, "Sampling from a System-Theoretic Viewpoint: Part I—Concepts and Tools, Part II—Noncausal Solutions", *IEEE Trans. On Signal Procesing*, Vol. 58, No. 7, pp. 3578–3606 (2010).

14. T. Kaczorek, *Control and systems theory* (in polish), Wyd. Naukowe PWN, W-wa , 1999.
15. M. Gwóźdź, “Impact of Aliasing Effect on Work of Wide Band Power Electronics Current Source”, *XIX Symposium Electromagnetic Phenomena in Nonlinear Circuits*, Maribor, Słowenia, 147-148 (2006).
16. M. Krystkowiak and M. Gwóźdź, “Calculation of Parameters of Equivalent Circuit of Pulse Transformer”, *XX Symposium Electromagnetic Phenomena in Nonlinear Circuits*, Lille, France, 139–140 (2008).
17. Product page of ALFINE-TIM: http://analog.alfine.pl/ [accessed: 04.2014].

***Autorzy**: dr hab. inż. Michał Gwóźdź, dr inż. Michał Krystkowiak; Instytut Elektrotechniki i Elektroniki Przemysłowej, Zakład Energoelektroniki i Sterowania, Wydział Elektryczny, Politechnika Poznańska, ul. Piotrowo 3a 37, 60-965 Poznań, e-mail: Michal.Gwozdz@put.poznan.pl, Michal.Krystkowiak@put.poznan.pl.*